

# Characterization of Neuropilin-1 Structural Features That Confer Binding to Semaphorin 3A and Vascular Endothelial Growth Factor 165\*

Received for publication, February 19, 2002  
Published, JBC Papers in Press, March 8, 2002, DOI 10.1074/jbc.M201681200

Chenghua Gu<sup>‡§</sup>, Brian J. Limberg<sup>¶</sup>, G. Brian Whitaker<sup>¶</sup>, Ben Perman<sup>‡</sup>, Daniel J. Leahy<sup>§</sup>,  
Jan S. Rosenbaum<sup>¶</sup>, David D. Ginty<sup>‡\*\*</sup>, and Alex L. Kolodkin<sup>‡‡</sup>

From the <sup>‡</sup>Department of Neuroscience, <sup>§</sup>Howard Hughes Medical Institute, and <sup>¶</sup>Department of Biophysics and Biophysical Chemistry, The Johns Hopkins University School of Medicine, Baltimore, Maryland 21205 and <sup>¶</sup>Procter & Gamble Pharmaceuticals, Mason, Ohio 45040

Neuropilin-1 (Npn-1) is a receptor for both semaphorin 3A (Sema3A) and vascular endothelial growth factor 165 (VEGF<sub>165</sub>). To understand the role Npn-1 plays as a receptor for these structurally and functionally unrelated ligands, we set out to identify structural features of Npn-1 that confer binding to Sema3A or VEGF<sub>165</sub>. We constructed Npn-1 variants containing deletions within the “a” and “b” domains of Npn-1. More than 16 variants were expressed in COS-1 cells and tested for alkaline phosphatase-Sema3A as well as alkaline phosphatase-VEGF<sub>165</sub> binding. Our results indicate that each of the two Npn-1 CUB domains and the amino-terminal coagulation factor V/VIII domain (CF V/VIII) are essential for Sema3A binding, but only the amino-terminal Npn-1 CF V/VIII domain is required for binding to VEGF<sub>165</sub>. Guided by the structure of the bovine spermadhesin CUB domain, point mutants targeting defined surfaces of the Npn-1 a1 CUB domain were generated and tested for Sema3A and VEGF<sub>165</sub> binding. One Npn-1 variant, Npn-1<sup>2ABC</sup>, exhibits complete loss of Sema3A binding while retaining normal VEGF<sub>165</sub> binding. Moreover, co-immunoprecipitation experiments show that Npn-1<sup>2ABC</sup> can form a signaling complex with the VEGF<sub>165</sub> signaling receptor KDR/VEGFR-2. These results establish the identity of contact sites between Npn-1 and its semaphorin ligands, and they provide a foundation for understanding how Npn-1 functions as a receptor for distinct classes of ligands *in vivo*.

A complex but ordered series of axon guidance decisions during development is critical for the establishment of nervous system structure and function (1). The vertebrate vascular network is similarly complex, with interconnecting conduits that extend throughout the body that are often in close anatomical proximity to nerve pathways (2). Recent evidence sug-

gests that at least some of the same ligand-receptor systems coordinate development of both the nervous system and the cardiovascular system. For example, Eph receptors and their ligands, the ephrins, were first characterized as mediators of repulsive guidance events crucial for correct navigation of neuronal growth cones and migrating neural crest cells (3, 4). Their unexpected role in blood vessel formation was revealed when mutant mice that lacked either ephrin B2 or its cognate receptor EphB4 were shown to die during embryogenesis due to cardiovascular dysfunction (5, 6). Consistent with this observation, *ephrin B2* and *EphB4* were shown to have a reciprocal expression patterns in arterial and venous endothelial cells (6).

Another example of a cell surface receptor whose function is required for development of both the cardiovascular and nervous systems is neuropilin-1 (Npn-1).<sup>1</sup> Npn-1 was first identified by a monoclonal antibody (called A5) isolated in a screen for cell surface proteins capable of mediating axon guidance decisions during neural development (7, 8). Since its original characterization, molecular, cellular, genetic, and biochemical analyses have shown that Npn-1 is a multifunctional 130-kDa transmembrane protein capable of binding to distinct ligands belonging to completely unrelated protein families: the semaphorins and VEGFs (9–11). Npn-1 can also serve as a heterophilic cell adhesion molecule *in vitro* (12, 13).

The semaphorins are a large family of proteins that function in axon guidance and cell migration. Class 3 semaphorins, which include the protein semaphorin 3A (Sema3A), are well characterized members of the semaphorin family. *In vitro* studies have demonstrated that Npn-1 is the ligand binding component of the Sema3A holoreceptor complex (9, 10). Npn-1 is expressed in specific classes of developing neurons and is required for repulsive axon guidance mediated by Sema3A (7–10, 13, 14). Recently, members of the plexin family of large multidomain transmembrane proteins have been shown to physically associate with Npn-1 and together form the functional Sema3A receptor (15, 16). The Npn-1-plexin A1 complex exhibits an enhanced binding affinity for Sema3A as compared with Npn-1 alone (15), and a mouse with a targeted deletion of one plexin, *PlexA3*, exhibits defects in class 3 semaphorin-mediated axon repulsion (17).

VEGF family members are critical regulators of vasculogenesis, angiogenesis, and vascular remodeling. The biological effects of VEGFs are mediated by the receptor tyrosine kinases Flt-1 (VEGFR-1), Flk-1/KDR (VEGFR-2), and VEGFR-3 (18,

\* This work was supported by National Institute of Mental Health Grant R01MH59199 (to D. D. G. and A. L. K.), the Howard Hughes Medical Institute (to D. J. L. and D. D. G.), the McKnight Endowment Fund for Neuroscience (to A. L. K.), and National Institutes of Health National Research Service Award 5F32NS11016–02 (to C. G.). The costs of publication of this article were defrayed in part by the payment of page charges. This article must therefore be hereby marked “advertisement” in accordance with 18 U.S.C. Section 1734 solely to indicate this fact.

\*\* To whom correspondence may be addressed: Dept. of Neuroscience, The Johns Hopkins University School of Medicine, 725 N. Wolfe St., Baltimore, MD 21205. E-mail: dginty@jhmi.edu.

‡‡ To whom correspondence may be addressed: Dept. of Neuroscience, The Johns Hopkins University School of Medicine, 725 N. Wolfe St., Baltimore, MD 21205. E-mail: kolodkin@jhmi.edu.

<sup>1</sup> The abbreviations used are: Npn-1, neuropilin-1; VEGF, vascular endothelial growth factor; Sema3A, semaphorin 3A; IP buffer, immunoprecipitation buffer; BSA, bovine serum albumin; AP, alkaline phosphatase.

19). Interestingly, select isoforms of the VEGF family, including *VEGF*<sub>165</sub>, also bind with high affinity to Npn-1 (11). Expression of Npn-1 in endothelial cells enhances both affinity labeling of *VEGF*<sub>165</sub> to *VEGFR-2* and *VEGF*<sub>165</sub>-induced endothelial cell chemotaxis (11, 20). Thus, Npn-1 acts as a *VEGF*<sub>165</sub> co-receptor that augments the ability of *VEGF*<sub>165</sub> to activate *VEGFR-2*. Npn-1 has also been shown to form a complex with *VEGFR-2* (21). Therefore, Npn-1 serves as a ligand-binding subunit in receptor complexes for structurally distinct ligands, the secreted semaphorins and *VEGF*<sub>165</sub>. Consistent with that idea, *npn-1* mutant mice exhibit defects in projections of spinal and cranial nerves, and they die during midgestation due to severe cardiovascular dysfunction (22, 23). Defects observed in these mice could result from a loss of semaphorin-Npn-1 and/or *VEGF*-Npn-1 signaling.

To dissect the molecular mechanisms that contribute to vascular and neuronal functions of Npn-1, we and others have sought to identify structural features of Npn-1 that confer binding to its ligands. Npn-1 has a large extracellular domain, a single transmembrane domain, and a very short cytoplasmic domain (24). The Npn-1 extracellular domain contains two domains with homology to complement components C1r and C1s (CUB domains, also called "a1" and "a2") at the amino terminus, followed by two coagulation factor V/VIII domains (CF V/VIII, also called "b1" and "b2"), and one C-terminal MAM (meprin, A5,  $\mu$ -phosphatase) domain (also called "c"). The secreted class 3 semaphorins contain three domains: a long amino-terminal semaphorin domain (sema), which is the signature domain of this family, an immunoglobulin (Ig) domain, and a positively charged carboxyl-terminal basic domain (25). Previous work has shown that the sema domain of *Sema3A* can bind to Npn-1 and that it is necessary for *Sema3A* repulsive activity on neurons. The *Sema3A* Ig-basic region alone cannot elicit biological activity, although it can bind to Npn-1 with a much lower affinity than the intact *Sema3A* protein (26, 27).

Each of the Npn-1 extracellular domains is required for biological activity mediated by *Sema3A* (28–30), but only the CUB domains are required for binding to the sema domain of *Sema3A*. (31). Moreover, a Npn-1 variant lacking both a1 and a2 CUB domains is incapable of binding to *Sema3A* but does bind to *VEGF*<sub>165</sub>. In contrast, deletion of both Npn-1 b domains abolishes binding of both *Sema3A* and *VEGF*<sub>165</sub> (31). These results suggest that the Npn-1 binding determinants for *Sema3A* and *VEGF*<sub>165</sub> may be distinct. Here we report the identification of amino acid residues within the Npn-1 CUB domains that are required for *Sema3A* binding but not *VEGF*<sub>165</sub> binding. We find that amino acid substitutions within two adjacent hydrophilic loops of the amino-terminal Npn-1 CUB domain dramatically reduce binding to class 3 semaphorins without affecting *VEGF*<sub>165</sub> binding. In addition to providing insight into the nature of the interactions between Npn-1 and its distinct ligands, these results establish a foundation for understanding how Npn-1 functions as a receptor for distinct classes of ligands *in vivo* and may also provide a basis for rational drug design.

#### EXPERIMENTAL PROCEDURES

**Neuropilin-1 Constructs**—Npn-1 deletion constructs for ligand-binding assays were created by inverse PCR using the ExSite kit (Stratagene). Full-length rat Npn-1 in the expression vector pMT21 served as a template for PCRs using oligonucleotide pairs that flanked the region of interest, including a1, a2, b1, and b2. The oligonucleotides contained a *SalI* restriction site at their 5'-ends. Following amplification, inverse PCR products were digested with *SalI* and circularized by ligation yielding Npn-1 deletion constructs:  $\Delta$  a1+7 (T30–145E),  $\Delta$  a2 (146C–274K),  $\Delta$  b1(275C–370P), and  $\Delta$  b2 (371C–587V). All cloning sites were sequenced, and the expression of correctly sized Npn-1 deletion mutants was confirmed by immunoblotting.

Npn-1 mutation constructs including Npn-1<sup>2I</sup>, Npn-1<sup>2AB</sup>, Npn-1<sup>2C</sup>,

Npn-1<sup>3D</sup>, and Npn-1<sup>2ABC</sup> were created by three PCR steps. Full-length Npn-1 in the expression vector pMT21 served as a template for the first two PCRs using two pairs of primers. The 5' primer from the first pair (nucleotides 6–18) includes a native *EcoRI* site. The 3' primer from the first pair and the 5' primer from the second pair overlap and include the introduced mutations. The 3' primer from the second pair of primers (nucleotides 2515–2539) contains a native *EcoRV* restriction site. The mixture of these first two purified PCR products then served as a template for the third PCR, using the 5' primer from the first pair and the 3' primer from the second pair. Following amplification, the third PCR product was double-digested with *EcoRI/EcoRV* and subsequently used to replace the corresponding region of wild type Npn-1 in pMT21. This yielded the following Npn-1 mutation constructs: Npn-1<sup>2I</sup>, Npn-1<sup>2AB</sup>, Npn-1<sup>2C</sup>, and Npn-1<sup>3D</sup>. Mutant Npn-1<sup>2ABC</sup> was created by using Npn-1<sup>2AB</sup> as a template for the first two PCRs, and the same primers were used for generating Npn-1<sup>2C</sup>. All PCR products and cloning sites were sequenced, and the expression of correctly sized Npn-1 mutants was confirmed by immunoblotting.

**Ligand Preparation**—AP-tagged ligands were produced in HEK 293T cells. DNA was introduced into cells by LipofectAMINE 2000 (Invitrogen). Conditioned medium was harvested 48 h posttransfection. Ligand concentration was determined as described (37), assuming a specific activity of 2000 units/mg. AP-*VEGF* cDNA was obtained from Dr. Michael Klagsbrun (Harvard Medical School). *VEGF*<sub>165</sub> used for *VEGFR-2* phosphorylation experiments was obtained from Sigma.

**Binding Assays**—AP-ligand binding assays were performed as described (31). Briefly, Npn-1 constructs were expressed in COS-1 cells following transfection using LipofectAMINE (Invitrogen). Forty-eight hours posttransfection, cells were incubated with various AP-tagged ligands or with anti-Npn-1 (anti-b2/c domains) (10) for cell surface expression. Bound AP activity values were normalized for protein concentration and Npn-1 cell surface expression levels. The normalized AP values for Npn-1 variants were then reported as percentage binding relative to wild-type Npn-1.

**Immunoprecipitation and Immunoblotting**—HEK 293T cells were co-transfected with an expression vector encoding Myc-Plex A1 (4  $\mu$ g; a gift from Dr. Stephen M. Strittmatter, Yale University) and an expression vector encoding various Npn-1 variants (4  $\mu$ g) using LipofectAMINE (Invitrogen). After 2 days, cells were lysed with ice-cold immunoprecipitation buffer (IP buffer; 50 mM Tris-HCl (pH 8.0), 1% Nonidet P-40, 2 mM EDTA, 0.5 mM polyvinylidene difluoride, 0.3  $\mu$ M aprotinin, and 10  $\mu$ M leupeptin). Insoluble proteins were removed by centrifugation at 10,000  $\times$  g for 10 min at 4 °C. The concentration of total soluble proteins was determined by the Bradford protein assay (Bio-Rad). Immunoprecipitations were performed using 0.5 mg of protein in a volume of 0.5 ml to which 2  $\mu$ l of anti-Myc (9E10) ascites was added. Immunocomplexes were recovered using an excess of protein G-Sepharose (Gammanbind; Amersham Biosciences). Following several washes in IP buffer, proteins were eluted in Laemmli sample buffer and then heated at 100 °C for 5 min. Proteins were electrophoresed through standard SDS-polyacrylamide gels and transferred to polyvinylidene difluoride membranes. Membranes were then blocked with TBS containing 0.5% nonfat dried milk and 0.1% Tween 20 and probed with anti-Npn-1 (10) polyclonal rabbit IgG (0.5  $\mu$ g/ml). Then blots were probed with peroxidase-conjugated donkey anti-rabbit Ig (Amersham Pharmacia Biotech) (1:5000), and bound secondary antibody was detected with a chemiluminescent peroxidase substrate (Super Signal; Pierce). The same blot was stripped with stripping buffer (62.5 mM Tris base, 2% SDS, and 0.7%  $\beta$ -mercaptoethanol) for 1 h at room temperature and reprobed with anti-Myc primary antibody (1:2000 dilution) and peroxidase-conjugated sheep anti-mouse (Amersham Biosciences) secondary antibody. Control lysates from matched samples were prepared without immunoprecipitation and processed identically as the immunoprecipitated samples described above using anti-Npn-1.

HEK 293T cells were transfected with expression vector for *VEGFR-2* (4  $\mu$ g; a gift from Dr. Cam Patterson, University of North Carolina), together with an expression vector for various Npn-1 constructs (4  $\mu$ g) by the LipofectAMINE method (Invitrogen). After 48 h, the cells were rinsed with Dulbecco's modified Eagle's medium, serum-starved (2–3 h, 37 °C), and then treated with 1 nM *VEGF* for 5 min at 37 °C. Cells were lysed with IP buffer containing sodium orthovanadate (1 mM), and the samples were immunoprecipitated with anti-Npn-1 (1  $\mu$ g/ml). Samples were then washed with IP buffer, resolved by SDS-PAGE, and transferred onto polyvinylidene difluoride membranes. The membranes were blocked with TBS containing 3% BSA, 1% normal donkey serum, and 0.1% Tween 20. The membranes were then probed with primary antibody 4G10 anti-phosphotyrosine (0.5  $\mu$ g/ml; Upstate Biotechnology Inc., Lake Placid, NY) and peroxidase-conjugated sheep

anti-mouse (Amersham Biosciences) secondary antibody. Membranes were stripped and reprocessed for VEGFR-2 normalization using the polyclonal Ab R2.2 (21).

**Cell Surface Binding Analysis and Immunocytochemistry**—COS-1 cells were transfected with 1  $\mu$ g of pMT21, pMT21-Npn-1, or pMT21-Npn-1<sup>2ABC</sup> using LipofectAMINE. After 48 h, cells were subjected either to cell surface binding analysis (37) or to cell surface Npn-1 immunocytochemistry. Immunocytochemistry was performed without fixation by incubating cells with blocking solution (5% goat serum in Dulbecco's modified Eagle's medium) for 20 min at 4 °C, followed by anti-Npn-1 (1:250 dilution in Dulbecco's modified Eagle's medium containing 2% goat serum) for 30 min at room temperature. Afterward, the cells were washed three times with PBS and fixed with 4% paraformaldehyde for 10 min at room temperature. The cells were washed with PBS an additional three times and incubated with secondary Oregon Green 488 goat anti-rabbit (Molecular Probes, Inc., Eugene, OR) at a dilution of 1:1000. Cells were then visualized under fluorescent microscopy.

**Iodination of VEGF<sub>165</sub>**—The iodination of VEGF<sub>165</sub> was performed as previously reported (21). Briefly, 5  $\mu$ g of carrier-free human recombinant VEGF<sub>165</sub> was suspended in 90  $\mu$ l of Dulbecco's phosphate-buffered saline. To the reaction tube, 1 mCi of Na<sup>125</sup>I was added, followed by 40  $\mu$ l of chloramine T (1  $\mu$ g/ $\mu$ l in 0.5 M sodium phosphate buffer, pH 7.5) and incubated for 1 min. 50  $\mu$ l of sodium metabisulfite (2  $\mu$ g/ $\mu$ l in sodium phosphate buffer, pH 7.5) was added to stop the reaction. 500  $\mu$ l of column elution buffer (0.5% BSA, 0.01% Tween 20 in Dulbecco's phosphate-buffered saline) was added to the reaction and transferred to preequilibrated PD-10 column for separation from unreacted iodine. The specific activity was corrected for column recovery and varied from 5,500 to 7,500 Ci/mmol.

**Saturation Analysis and Nonlinear Curve Fitting**—The saturation analysis was performed as previously reported (21). Briefly, COS-1 cells transiently expressing either the Npn-1 or the Npn-1<sup>2ABC</sup> mutant receptor were plated at  $2 \times 10^5$  cells/well in a 12-well plate 24 h prior to experimentation. The following morning, the cells were rinsed with 1 ml of binding buffer (Dulbecco's modified Eagle's medium, 0.2% BSA, 25 mM HEPES) and were preequilibrated in the same buffer for 1 h at 4 °C. Increasing concentrations (30–5000 pM) of [<sup>125</sup>I]VEGF<sub>165</sub> were added in binding buffer containing a protease inhibitor mixture (final concentration as follows: leupeptin, 10  $\mu$ g/ml; antipain, 10  $\mu$ g/ml; aprotinin, 50  $\mu$ g/ml; benzamide, 100  $\mu$ g/ml; soybean trypsin inhibitor, 100  $\mu$ g/ml; bestatin, 10  $\mu$ g/ml; pepstatin 10  $\mu$ g/ml; phenylmethylsulfonyl fluoride, 0.3 mM) and 1  $\mu$ g/ml heparin in the presence or absence of 30 nM unlabeled VEGF<sub>165</sub> to estimate nonspecific binding. The nonspecific binding was linear over the indicated tracer concentration range (data not shown). The binding reaction was allowed to reach equilibrium (4 h at 4 °C), and the unbound ligand was removed by washing three times (1 ml) with ice-cold BSA-free binding buffer. The cells were lysed with 250  $\mu$ l of RIPA buffer (20 mM Tris-HCl, pH 7.4, 100 mM NaCl, 1 mM EDTA, 10 mM NaI, 0.5% Nonidet P-40, 0.5% sodium deoxycholate, 1% BSA, 0.1% SDS) and counted using a  $\gamma$ -counter. The maximum number of binding sites ( $B_{max}$ ) and the equilibrium dissociation constant ( $K_d$ ) values were obtained using the Prism software package, which performs a statistical assessment of goodness of fit to a one-binding site versus a two-binding site model. This methodology is preferred over the Scatchard analysis, since it does not require a transformation and linearization of the data, which is known to distort the experimental errors associated with radioligand-binding data (38). In all cases described herein, the optimal fit of the data was to a one-binding site model (data not shown). The data points in all curves were determined in triplicate. The lower  $B_{max}$  value observed for the mutant receptor (as compared with the wild type receptor; see Table I) can be attributed to the lower expression level of mature protein for the mutant receptor in the COS-1 transient expression system (data not shown).

**Modeling/Solvent Exposure**—The bovine spermadhesin CUB domain was displayed, and side chain was changed to the corresponding residues in Npn-1 using the program O (39). Fractional solvent accessibilities were calculated using the program X-PLOR (40).

## RESULTS

**Binding Domains of Npn-1 for VEGF<sub>165</sub> and Sema3A Are Distinct**—We set out to identify structural features of Npn-1 that confer binding to VEGF<sub>165</sub> and Sema3A, two structurally unrelated ligands with distinct functions. Using a PCR-based mutagenesis approach, we constructed a battery of Npn-1 variants harboring different deletions within the CUB and CF-V/VIII domains. Npn-1 variants lacking individual CUB (a1 or

a2) or CF-V/VIII (b1 or b2) domains were generated (Fig. 1A) and expressed in COS-1 cells. Expression of these variants was confirmed by anti-Npn-1 Western blots and cell surface immunostaining in the absence of detergent. Each variant was tested for its ability to bind to Sema3A and VEGF<sub>165</sub> ligands fused at their N termini to alkaline phosphatase (AP-Sema3A and AP-VEGF<sub>165</sub>). Both of these AP fusion proteins bind with high affinity to Npn-1 (10, 20). Fig. 1 depicts four of the Npn-1 deletion variants and their AP-Sema3A and AP-VEGF<sub>165</sub> binding properties. Deletion of either the a1 or a2 CUB domains abolished AP-Sema3A binding but had relatively little effect on VEGF<sub>165</sub> binding (Fig. 1, C and D). In contrast, deletion of the b1 CF-V/VIII domain abolished binding to both ligands (Fig. 1, C and D). Deletion of the b2 CF-V/VIII domain did not abolish binding to either ligand (Fig. 1, C and D), although reduced binding of AP-VEGF<sub>165</sub> to the b2 deletion variant was consistently observed. These results suggest that each of the CUB domains is essential for Sema3A but not VEGF<sub>165</sub> binding, and the b1 CF-V/VIII region is required for binding to both ligands.

**Mutations in Two a1 CUB Domain Loop Regions Completely Abolish AP-Sema-Fc Binding without Affecting AP-VEGF<sub>165</sub> Binding**—To further refine our characterization of distinct ligand-binding sites on Npn-1, candidate Sema3A-binding residues were sought by generating a three-dimensional model of the Npn-1 a1 CUB domain. Using the crystal structure of the bovine spermadhesin CUB domain (32) and an alignment of the Npn-1 a1 and spermadhesin CUB domain amino acid sequences, we identified four loop regions in the Npn-1 a1 CUB domain that are likely to be solvent-exposed (Fig. 2, labeled red (2I), pink (2AB), light green (2C), and dark green (3D)). Three of these (2AB, 2C, and 3D) reside on one side of the predicted a1 CUB domain, whereas the fourth (2I) lies on the opposite side. Solvent-exposed regions were sought because they are likely to mediate interactions with ligands, and mutations at such sites are less likely to disrupt global structure. Residues of the four regions selected for mutation (2A, 2B, 2C, and 2I) were not only solvent-exposed but were also different, based on their sequence alignment, from the corresponding neuropilin-2 amino acids. New variants harboring substitutions of either two or three amino acids in each of these four regions (Npn-1<sup>2I</sup>, Npn-1<sup>2AB</sup>, Npn-1<sup>2C</sup>, and Npn-1<sup>3D</sup>) were generated. Charged residues were substituted with oppositely charged residues in these variants, as shown in Fig. 2B. These four Npn-1 variants were subsequently tested for their ability to bind Npn-1 ligands.

Npn-1<sup>2I</sup>, Npn-1<sup>2AB</sup>, Npn-1<sup>2C</sup>, and Npn-1<sup>3D</sup> were each expressed in transfected COS-1 cells (Fig. 3A). Whole cell binding assays were performed using these variants and wild type Npn-1 (Fig. 3B). AP-Sema-Fc, a fusion protein in which the Sema3A Ig and basic domains were replaced by the immunoglobulin Fc domain (31), was used in these assays instead of an AP-Sema3A protein. This was done to eliminate any binding contribution of the Sema3A Ig region to the Npn-1 b1 CF-V/VIII domain, an interaction that in the absence of the Sema3A sema domain does not result in signaling.

Interestingly, the three variants having substitutions residing on the same face of the predicted a1 CUB domain (Npn-1<sup>2AB</sup>, Npn-1<sup>2C</sup>, and Npn-1<sup>3D</sup>) each exhibited dramatically reduced levels of AP-Sema-Fc binding, whereas Npn-1<sup>2I</sup>, which has substitutions located on the opposite side of the a1 CUB domain, did not exhibit altered AP-Sema-Fc binding (Fig. 3B). Therefore, we postulated that the natural residues on adjacent loop regions might coordinately interact with the sema domain of Sema3A. To test this idea, an additional Npn-1 variant, Npn-1<sup>2ABC</sup>, was generated by combining the 2AB and 2C substitutions. Npn-1<sup>2ABC</sup> contains a five-amino acid substitution

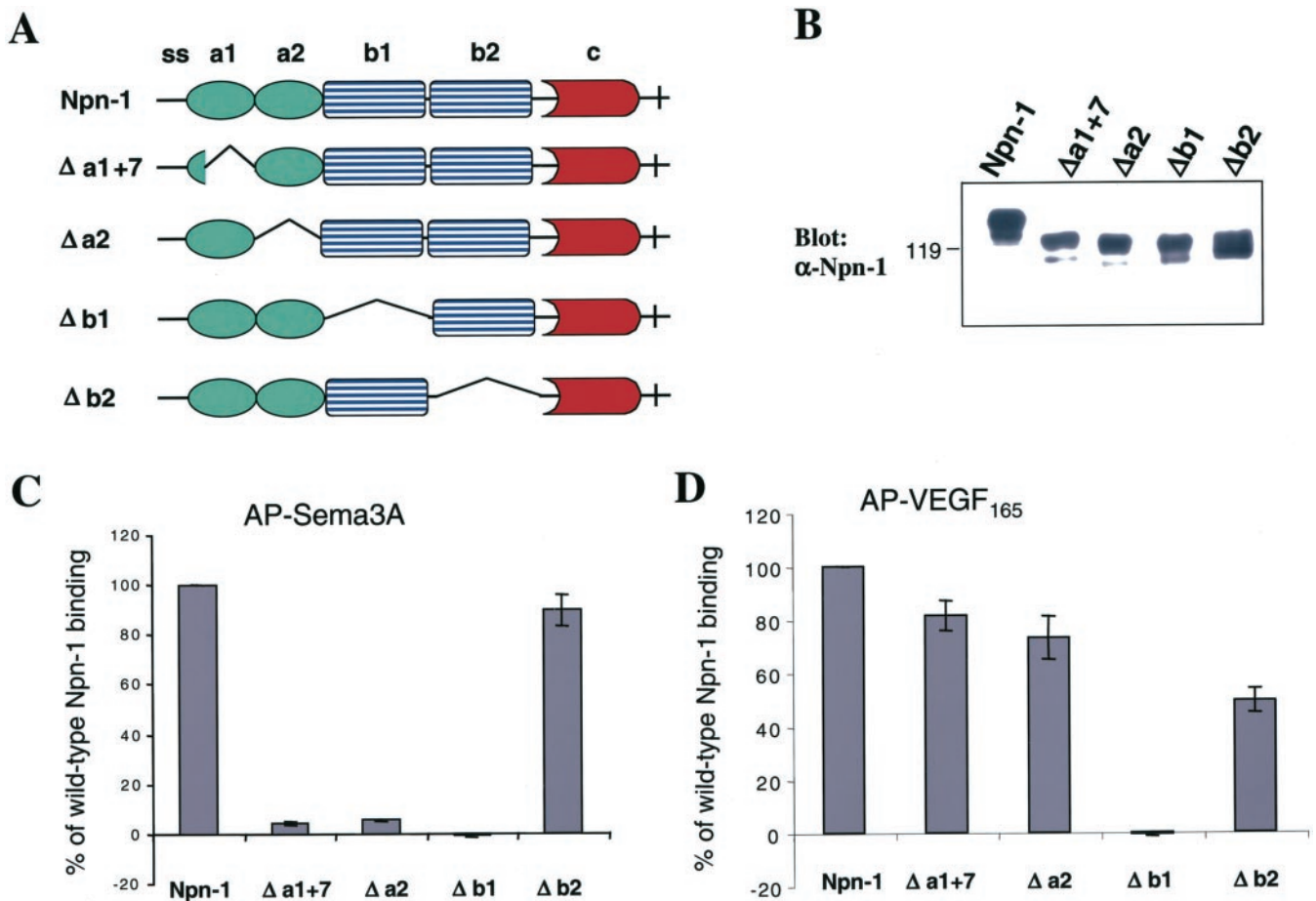


**FIG. 1. The Neuropilin-1 a (CUB) and b (CF V/VIII) domains differentially confer *Sema3A* and *VEGF*<sub>165</sub> binding.** *A*, schematic representation of neuropilin-1 (Npn-1) and Npn-1 deletion mutants. *B*, Western blot analysis of expression of wild type and various neuropilin-1 deletion mutants in transfected COS-1 cells. Immunoblot with anti-Npn-1 demonstrates comparable expression levels of all variants. *C*, quantitation of AP-*Sema3A* binding to full-length Npn-1 and Npn-1 deletion mutants. Full-length Npn-1 and deletion mutants were expressed in COS-1 cells. The bound AP activity values were obtained using whole-cell AP-*Sema3A* (4 nM) and AP-*VEGF*<sub>165</sub> (4 nM) binding assays. The bound AP activities were normalized for protein concentration and cell surface expression of Npn-1 proteins. The normalized AP values of different deletion mutants were then compared with full-length Npn-1, here presented as percentage of binding compared with wild-type Npn-1. *D*, quantitation of AP-*VEGF*<sub>165</sub> binding to full-length Npn-1 and Npn-1 deletion mutants. Shown are the means  $\pm$  S.E. from three separate binding experiments.

in one surface loop and a two-amino acid substitution in the adjacent loop on the same face of the a1 CUB domain (Fig. 2B). Although Npn-1<sup>2ABC</sup> was expressed in COS cells at levels similar to wild-type Npn-1 (Fig. 3A), its binding to AP-*Sema3A* was undetectable in the solution AP activity assay (Fig. 3B). Cell surface binding of AP-*Sema3A*, AP-*VEGF*<sub>165</sub>, and AP-*Sema3A* to Npn-1<sup>2ABC</sup>-expressing COS-1 cells was also visualized by alkaline phosphatase histochemical staining (Fig. 3C). There was a complete absence of AP-*Sema3A* and AP-*Sema3A* staining in Npn-1<sup>2ABC</sup>-expressing COS cells (Fig. 3C, *f* and *i*), although Npn-1<sup>2ABC</sup> is expressed on the plasma membrane as determined by immunostaining with anti-Npn-1 in living cells (Fig. 3C, *c*). The binding of AP-*VEGF*<sub>165</sub> to Npn-1<sup>2ABC</sup>-expressing cells appeared normal (Fig. 3C, *i*). To confirm that Npn-1<sup>2ABC</sup> exhibits normal, high affinity *VEGF*<sub>165</sub> binding, we performed a saturation binding analysis of *VEGF*<sub>165</sub> for wild-type Npn-1 and Npn-1<sup>2ABC</sup>. For these experiments, wild-type Npn-1 and Npn-1<sup>2ABC</sup> were transiently expressed in COS-1 cells, and whole cell saturation analyses using [<sup>125</sup>I]*VEGF*<sub>165</sub> were performed 2 days later. The calculated  $K_d$  for Npn-1<sup>2ABC</sup> is 1.48 nM, which is approximately equivalent to that of wild type Npn-1 ( $K_d = 0.93$  nM) (Fig. 3D). The lower  $B_{max}$  value obtained for *VEGF*<sub>165</sub> binding to Npn-1<sup>2ABC</sup> is the result of lower expression levels of Npn-1<sup>2ABC</sup> in these binding experiments (data not shown). Therefore, the 2ABC mutations define a1 CUB domain

loop regions that are required for *Sema3A* but not *VEGF*<sub>165</sub> binding to Npn-1.

**Mutation 2ABC Abolishes Npn-1 Binding to Other Class 3 Semaphorins**—In addition to *Sema3A*, other class 3 semaphorins, including *Sema3F* and *Sema3C*, can bind to Npn-1 (27). Therefore, whole cell binding experiments were performed using AP-*Sema3A*, AP-*Sema3C*, and AP-*Sema3F* to determine whether the Npn-1 2ABC region is required for binding to these class 3 semaphorins. In these assays, Npn-1<sup>2ABC</sup> exhibited markedly reduced binding to each of the class 3 semaphorins tested (Fig. 4). *Sema3A*, *Sema3C*, and *Sema3F* binding to Npn-1 was affected to a similar extent by the 2ABC mutation. The small amount of residual binding of these semaphorin ligands to Npn-1<sup>2ABC</sup> may result from an interaction between the carboxyl-terminal immunoglobulin and/or basic regions of class 3 semaphorins and the b1 CF-V/VIII domain of Npn-1. Thus, the sema domains of the different class 3 semaphorins bind to the same surface region of Npn-1.

**Npn-1<sup>2ABC</sup> Exhibits Normal Binding to Plexin A1 and *VEGFR-2***—In addition to its ability to bind structurally distinct ligands, Npn-1 directly interacts with multiple transmembrane signal-transducing receptor subunits. Members of the plexin family of transmembrane proteins are signal-transducing subunits of holoreceptors for class 3 semaphorins, whereas *VEGFR-2* is a signaling receptor for *VEGF*<sub>165</sub> (19, 26). Both

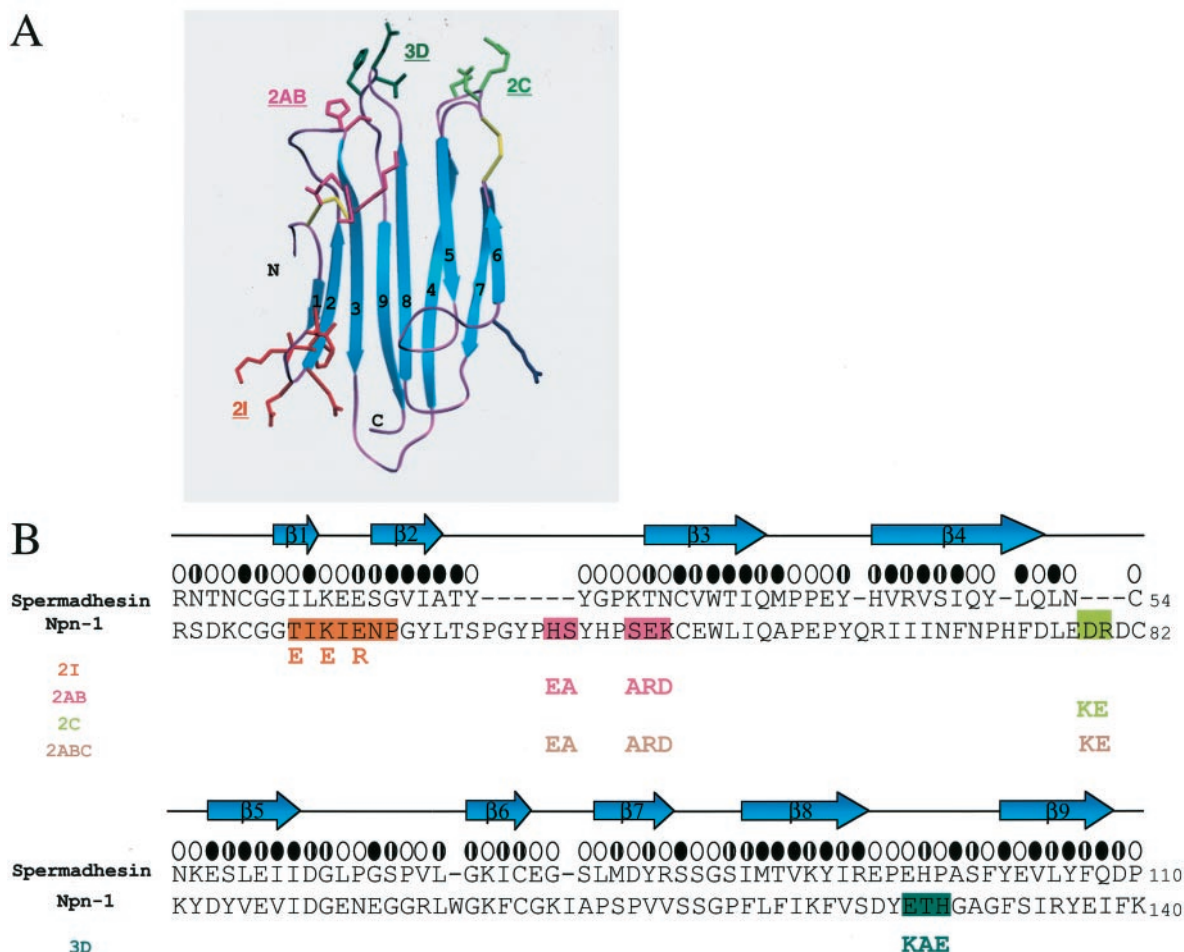


FIG. 2. Sites of Npn-1 mutations on a ribbon diagram of the bovine spermadhesin CUB domain. *A*, side chains of bovine spermadhesin were changed to the corresponding Npn-1 residues and displayed on a ribbon diagram of the bovine spermadhesin CUB domain. The ribbon diagram was generated with program SETOR (41). *B*, a structure-guided alignment of the bovine spermadhesin and Npn-1 a1 CUB domain. Positions of the spermadhesin  $\beta$ -strands are indicated, and buried residues (FSA  $\leq 0.1$ ) are indicated by filled ovals, exposed residues (FSA  $\geq 0.4$ ) are indicated by open ovals, and partially buried residues (FSA = 0.1–0.4) are indicated by half-filled ovals.

plexin A1 and VEGFR-2 form complexes with Npn-1 in a ligand-independent manner. The regions of interaction between Npn-1 and plexin A1 as well as Npn-1 and VEGFR-2 are not yet established. It is interesting to note that plexins have sema domains distantly related to the sema domains of the semaphorin ligands, and it is possible that the Npn-1 CUB domains interact with the sema domains of both the secreted semaphorins and plexins. Therefore, we next sought to establish whether the 2ABC surface of the Npn-1 a1 CUB domain contributes to the association between Npn-1 and either plexin A1 or VEGFR-2.

We performed a coimmunoprecipitation assay to compare the abilities of wild-type Npn-1 and Npn-1<sup>2ABC</sup> to associate with plexin A1. Wild-type Npn-1 and the Npn-1<sup>2ABC</sup> variant were co-expressed with Myc-tagged plexin A1 in HEK293T cells, and complexes were immunoprecipitated using anti-Myc. Anti-Npn-1 immunoblots of the anti-Myc immune complexes demonstrated that comparable amounts of Npn-1 and Npn-1<sup>2ABC</sup> co-precipitated with Myc-plexin A1 (Fig. 5A). Reprobing the same blot with anti-Myc showed equal amounts of plexin A1 in the complexes (Fig. 5B). Moreover, levels of expression of Npn-1 and Npn-1<sup>2ABC</sup> were similar (Fig. 5C). Therefore, in contrast to its role in binding to the sema domain of class 3 semaphorins, the 2ABC surface region of Npn-1 is not required for its association with plexin A1.

Npn-1 and VEGFR-2 form a complex in transfected COS-1 cells as well as in cultured endothelial cells, and this complex is

responsible for the different relative potencies of VEGF isoforms in VEGFR-2 autophosphorylation assays (21). To determine whether the 2ABC surface of the Npn-1-VEGFR-2 complex contributes to the formation of the Npn-1-VEGFR-2 complex or VEGF<sub>165</sub>-mediated VEGFR-2 phosphorylation, additional cotransfection experiments were performed. Wild-type Npn-1 and Npn-1<sup>2ABC</sup> were co-expressed with VEGFR-2 in HEK293T cells. Cells were treated with VEGF<sub>165</sub> (1 nM) for 5 min and then lysed. Cell extracts were immunoprecipitated with anti-Npn-1, and immune complexes were blotted with anti-phosphotyrosine (Fig. 6A). VEGF<sub>165</sub> treatment resulted in similar levels of tyrosine-phosphorylated VEGFR-2 detected in Npn-1 immune complexes obtained from Npn-1 and Npn-1<sup>2ABC</sup>-expressing cells (Fig. 6A). The tyrosine-phosphorylated bands were shown to be VEGFR-2 by reprobing the blot with anti-VEGFR-2 (Fig. 6B). Importantly, levels of expression of Npn-1 and Npn-1<sup>2ABC</sup> were similar in the matched lysates (Fig. 6C). Therefore, the 2ABC mutation affected neither VEGF<sub>165</sub> ligand binding nor Npn-1/VEGFR-2 association. Furthermore, the ability of VEGF<sub>165</sub> to induce VEGFR-2 autophosphorylation within the VEGFR-2-Npn-1 complex was unaltered by the 2ABC mutation.

#### DISCUSSION

Guided by the structure of the bovine spermadhesin CUB domain (32), we have identified seven amino acids located on two adjacent hydrophilic loops of the amino-terminal Npn-1

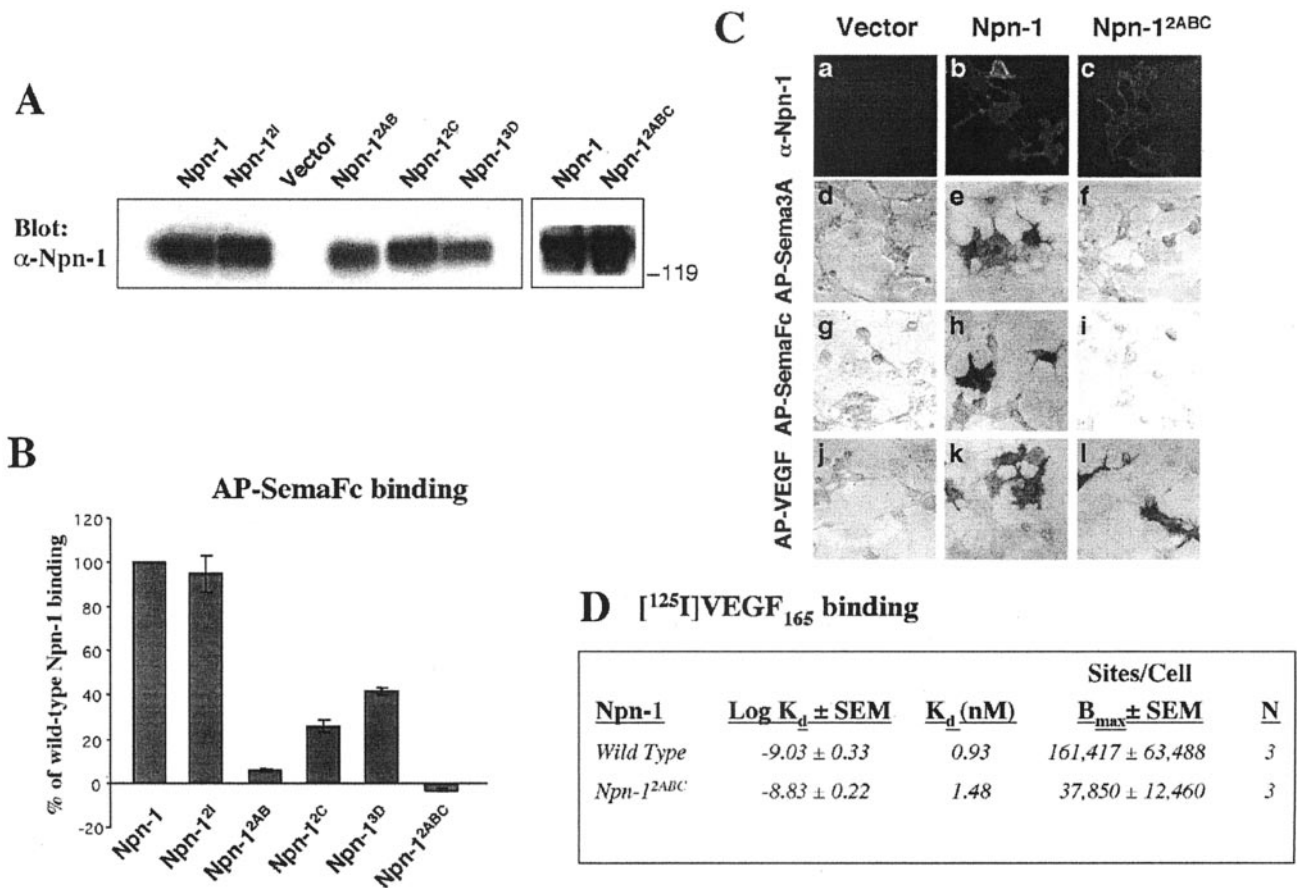


**FIG. 3. Point mutations on the predicted surface loops of the Npn-1 a1 CUB domain differentially affect *Sema3A* and *VEGF*<sub>165</sub> binding.** *A*, Western blot analysis of COS-1 cell expression of wild-type and various Npn-1 side chain mutants. Immunoblot with anti-Npn-1 shows comparable expression levels of all variants. *B*, quantitation of the sema domain of *Sema3A* (AP-SemaFc) (7 nM) binding to wild-type Npn-1 and Npn-1 variants harboring various a1 CUB domain side chain mutations. *C*, cell surface expression and ligand binding of Npn-1 and Npn-1<sup>2ABC</sup>. COS-1 cells were transiently transfected with expression vectors encoding either Npn-1 (*b*, *e*, *h*, and *k*), Npn-1<sup>2ABC</sup> (*c*, *f*, *i*, and *l*), or vector alone (*a*, *d*, *g*, and *j*). Binding of full-length *Sema3A* (AP-Sema3A) (*d*–*f*), the sema domain of *Sema3A* (AP-SemaFc) (*g*–*i*), and *VEGF*<sub>165</sub> (AP-VEGF) (*j*–*l*) was visualized by alkaline phosphatase histochemistry. Note that there is no binding of the full-length or sema domain of *Sema3A* to Npn-1<sup>2ABC</sup> despite expression of the protein on the cell surface (*c*). In contrast, *VEGF*<sub>165</sub> does bind Npn-1<sup>2ABC</sup> (*l*). *a*–*c*, immunostaining of cell surface wild type and Npn-1<sup>2ABC</sup> in living (nonpermeabilized) cells with anti-Npn-1 polyclonal antibodies. *D*, [<sup>125</sup>I]*VEGF*<sub>165</sub> binding parameters for wild type Npn-1 and Npn-1<sup>2ABC</sup> variant. Dissociation constant ( $K_d$ ) and the predicted maximum number of binding sites ( $B_{max}$ ) values were determined using saturation binding and nonlinear curve fitting analyses. Shown are means  $\pm$  S.E. for three separate experiments. The lower  $B_{max}$  value observed for Npn-1<sup>2ABC</sup> is due to the lower expression levels of Npn-1<sup>2ABC</sup> in the COS-1 transient expression system (data not shown).

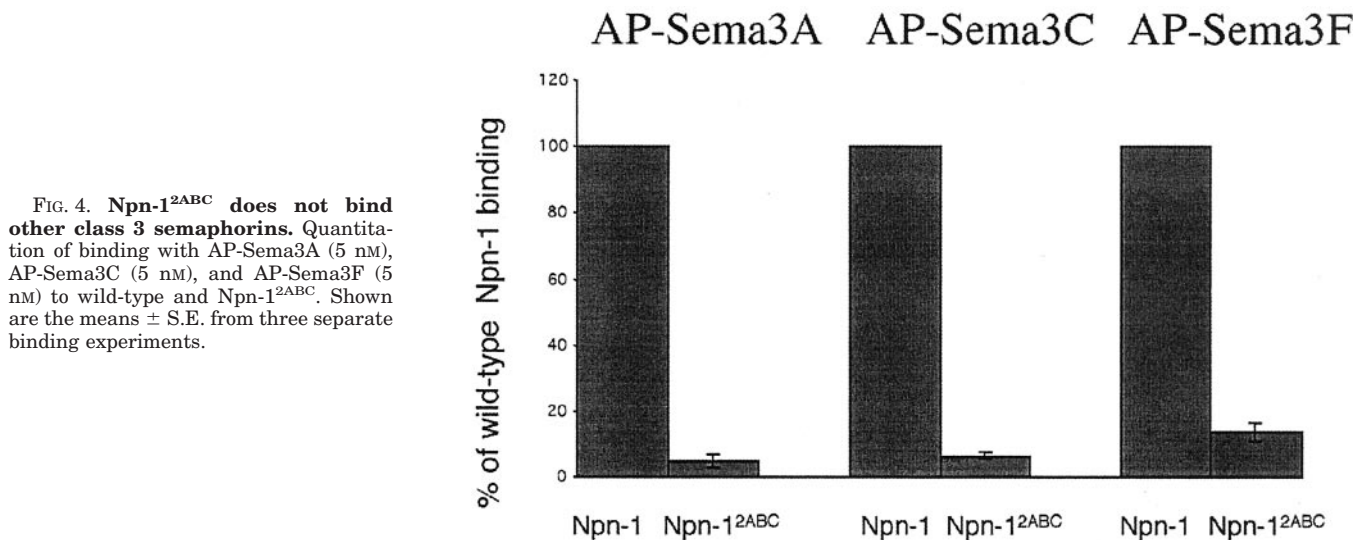


**FIG. 4. Npn-1<sup>2ABC</sup> does not bind other class 3 semaphorins.** Quantitation of binding with AP-Sema3A (5 nM), AP-Sema3C (5 nM), and AP-Sema3F (5 nM) to wild-type and Npn-1<sup>2ABC</sup>. Shown are the means  $\pm$  S.E. from three separate binding experiments.

CUB domain that are critical for binding to the sema domain of class 3 semaphorins. This surface region does not contribute to the binding of a structurally unrelated Npn-1 ligand, *VEGF*<sub>165</sub>,

nor is it required for association between Npn-1 and two of its signaling partners, plexin A1 and *VEGFR*-2. The identification of Npn-1 residues that comprise binding sites for distinct li-

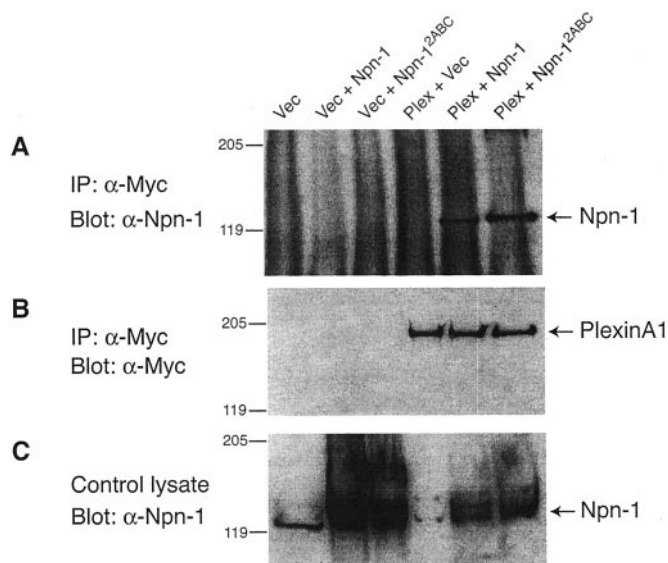


**FIG. 5. Npn-1<sup>2ABC</sup> forms a normal complex with its co-receptor plexin A1.** HEK293T cells were transfected with Npn-1, Npn-1<sup>2ABC</sup>, or vector together with Myc-tagged plexin A1. Cell lysates were subjected to immunoprecipitation using anti-Myc and blotted with anti-Npn-1 (A). The same blot was stripped and reblotted with anti-Myc (B). Lysates from the same set of samples used for immunoprecipitation were resolved by SDS-PAGE and immunoblotted with anti-Npn-1 (C). This experiment was done three times with similar results.

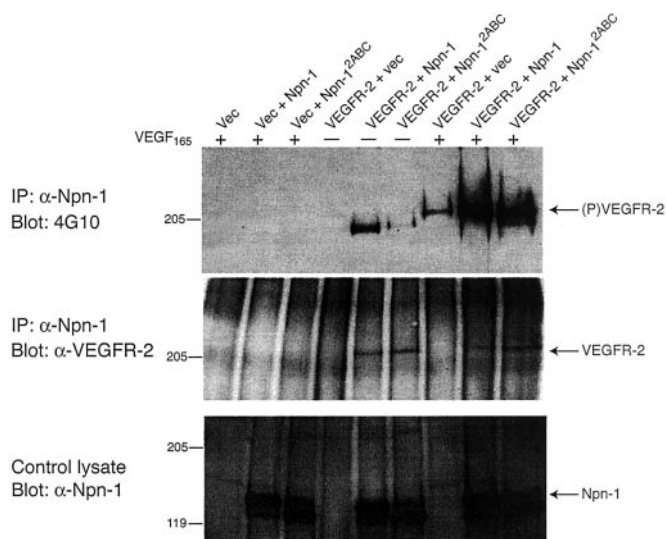


**FIG. 6. Association of Npn-1<sup>2ABC</sup> with VEGFR-2 is normal, as is its ability to mediate VEGF<sub>165</sub>-dependent phosphorylation of VEGFR-2.** HEK293T cells were transfected with expression vectors encoding either Npn-1, Npn-1<sup>2ABC</sup>, or vector together with vectors encoding VEGFR-2. Cells were treated with VEGF<sub>165</sub> (1 nM) or vehicle for 5 min and then lysed. Cell lysates were subjected to immunoprecipitation using anti-Npn-1 and blotted with anti-phosphotyrosine (4G10) (A) or anti-VEGFR-2 (B). Lysates from the same set of samples used for immunoprecipitation were resolved by SDS-PAGE and immunoblotted with anti-Npn-1 (C). Note that VEGF<sub>165</sub> induced similar levels of VEGFR-2 phosphorylation in VEGFR-2/Npn-1-expressing cells and VEGFR-2/Npn-1<sup>2ABC</sup>-expressing cells. This experiment was done three times with similar results.

gands should facilitate elucidation of the *in vivo* functions of Npn-1 as a receptor for distinct ligands and, possibly, the design of useful modulators or inhibitors of semaphorin/Npn-1 signaling.

The finding that Npn-1<sup>2ABC</sup> associates normally with plexin A1 is interesting, because, like the semaphorin ligands, plexins contain sema domains that can bind to Npn-1 (15, 16, 33). While it is not known whether plexin sema domains interact

with Npn-1 CUB domains, our results indicate that the 2ABC surface of the Npn-1 a1 CUB domain is not an obligatory site of contact between plexin A1 and Npn-1. Indeed, previous findings have indicated that multiple Npn-1 domains contribute to the Npn-1-plexin A1 association (15). Since multiple Npn-1 extracellular domains also appear to contribute to Npn-1 homomultimerization and heteromultimerization with neuropilin-2 (29, 31), and since the Npn-1 CUB domains are dispensable for Npn-1 multimerization, it is likely that Npn-1<sup>2ABC</sup> retains the capacity to form homo- and heteromultimers. Moreover, examination of the CUB domain dimer of major seminal plasma glycoproteins I and II (1SPP.pdb) reveals that the 2ABC region is not part of the dimer interface (32).

Npn-1 appears to be a remarkably versatile protein, because it serves as a binding subunit of receptor complexes for members of structurally distinct ligand families, the semaphorins and the VEGFs. The *in vivo* function of Npn-1 as the obligate ligand binding subunit of the *Sema3A* holoreceptor is well established (22, 26, 27). However, the role of Npn-1 as a necessary co-receptor for VEGF<sub>165</sub> signaling during development of the cardiovascular system is less clear. Expression of Npn-1 in vascular endothelial cells enhances both the affinity labeling of VEGF<sub>165</sub> to VEGFR-2 and VEGF<sub>165</sub>-induced cell chemotaxis (11, 20). Other recent studies have shown that Npn-1 does not augment VEGF<sub>165</sub>'s ability to bind to VEGFR-2 but rather increases its ability to promote autophosphorylation of VEGFR-2 (21). It is also possible that *Sema3C*-Npn-1 signaling is required for proper cardiac neural crest cell migration into the proximal cardiac outflow tract during development (34). Therefore, the cardiovascular defects in *nfn-1* null mice may be the result of a deficiency in semaphorin-Npn-1 signaling, VEGF-Npn-1 signaling or, perhaps most likely, both. Another striking feature of the *nfn-1* null mouse is the severe impairment of vascularization of the developing nervous system (22). Thus, Npn-1 may transmit semaphorin and/or VEGF family member signals within vascular endothelial cells to promote neovascularization of the developing nervous system.

VEGF and semaphorins may also have antagonistic effects on both neurons and vascular endothelial cells. VEGF<sub>165</sub> and *Sema3A* compete with each other in an endothelial motility assay, for sensory neuron growth cone collapse, and also in their ability to bind to Npn-1 (20). VEGF<sub>165</sub> can also antagonize *Sema3A*-induced apoptosis of neurons (35). Finally, VEGF<sub>165</sub> promotes growth of DRG sensory neuron axons, whereas *Sema3A* induces DRG axon repulsion and growth cone collapse (36). Thus, the precise roles of semaphorin-Npn-1 signaling, VEGF-Npn-1 signaling, and antagonistic interactions between Npn-1 ligands may be difficult to glean from simple comparisons between *nfn-1* null mice and mice harboring null mutations in genes encoding Npn-1 ligands. Our identification of Npn-1 variants that are defective in semaphorin-Npn-1 but not VEGF<sub>165</sub>-Npn-1 binding and signaling and our current analysis of the phenotype of mice harboring the 2ABC mutation introduced into the *nfn-1* locus should help to establish the *in vivo* roles of Npn-1 as a multifunctional and versatile receptor. The identification of subtle mutations in the Npn-1 b1 CF-V/VIII region, which serves as the binding site for VEGF<sub>165</sub>, should provide a reciprocal tool for establishing the *in vivo* roles of VEGF-Npn-1 interactions.

**Acknowledgments**—We thank Andrea Huber-Broesamle and Dori Reimert for comments on the manuscript, Dori Reimert for excellent technical assistance, and members of the Ginty and Kolodkin laboratories for helpful discussions. We thank M. Klagsbrun for the AP-VEGF construct, S. Strittmatter for the Myc-plexin A1 construct, and C. Patterson for the VEGFR-2 expression construct.

## REFERENCES

1. Tessier-Lavigne, M., and Goodman, C. S. (1996) *Science* **274**, 1123–1133
2. Shima, D. T., and Mailhos, C. (2000) *Curr. Opin. Genet. Dev.* **10**, 536–542
3. Holder, N., and Klein, R. (1999) *Development* **126**, 2033–2044
4. Wilkinson, D. G. (2000) *Int. Rev. Cytol.* **196**, 177–244
5. Gerety, S. S., Wang, H. U., Chen, Z. F., and Anderson, D. J. (1999) *Mol. Cell* **4**, 403–414
6. Wang, H. U., Chen, Z. F., and Anderson, D. J. (1998) *Cell* **93**, 741–753
7. Takagi, S., Tsuji, T., Amagai, T., Takamatsu, T., and Fujisawa, H. (1987) *Dev. Biol.* **122**, 90–100
8. Takagi, S., Hirata, T., Agata, K., Mochii, M., Eguchi, G., and Fujisawa, H. (1991) *Neuron* **7**, 295–307
9. He, Z., and Tessier-Lavigne, M. (1997) *Cell* **90**, 739–751
10. Kolodkin, A. L., Levengood, D. V., Rowe, E. G., Tai, U.-T., Giger, R. J., and Ginty, D. D. (1997) *Cell* **90**, 753–762
11. Soker, S., Takashima, S., Miao, H.-Q., Neufeld, G., and Klagsbrun, M. (1998) *Cell* **92**, 735–745
12. Shimizu, M., Murakami, Y., Suto, F., and Fujisawa, H. (2000) *J. Cell Biol.* **148**, 1283–1293
13. Takagi, S., Kasuya, Y., Shimizu, M., Matsuura, T., Tsuboi, M., Kawakami, A., and Fujisawa, H. (1995) *Dev. Biol.* **170**, 207–222
14. Kawakami, A., Kitsukawa, T., Takagi, S., and Fujisawa, H. (1996) *J. Neurobiol.* **29**, 1–17
15. Takahashi, T., Fournier, A., Nakamura, F., Wang, L.-H., Murakami, Y., Kalb, R. G., Fujisawa, H., and Strittmatter, S. M. (1999) *Cell* **99**, 59–69
16. Tamagnone, L., Artigiani, S., Chen, H., He, Z., Ming, G.-L., Song, H.-J., Chedotal, A., Winberg, M. L., Goodman, C. S., Poo, M.-M., Tessier-Lavigne, M., and Comoglio, P. M. (1999) *Cell* **99**, 71–80
17. Cheng, H. J., Bagri, A., Yaron, A., Stein, E., Pleasure, S. J., and Tessier-Lavigne, M. (2001) *Neuron* **32**, 249–263
18. Ferrara, N. (2001) *Am. J. Physiol.* **280**, C1358–C1366
19. Neufeld, G., Cohen, T., Gengrinovitch, S., and Poltorak, Z. (1999) *FASEB J.* **13**, 9–22
20. Miao, H.-Q., Soker, S., Feiner, L., Alonso, J. L., Raper, J. A., and Klagsbrun, M. (1999) *J. Cell Biol.* **146**, 233–241
21. Whitaker, G. B., Limberg, B. J., and Rosenbaum, J. S. (2001) *J. Biol. Chem.* **276**, 25520–25531
22. Kawasaki, T., Kitsukawa, T., Bekku, Y., Matsuda, Y., Sanbo, M., Yagi, T., and Fujisawa, H. (1999) *Development* **126**, 4895–4902
23. Kitsukawa, T., Shimizu, M., Sanbo, M., Hirata, T., Taniguchi, M., Bekku, Y., Yagi, T., and Fujisawa, H. (1997) *Neuron* **19**, 995–1005
24. Fujisawa, H., Kitsukawa, T., Kawakami, A., Takagi, S., Shimizu, M., and Hirata, T. (1997) *Cell Tissue Res.* **290**, 465–470
25. Semaphorin Nomenclature Committee (1999) *Cell* **97**, 551–552
26. Nakamura, F., Kalb, R. G., and Strittmatter, S. M. (2000) *J. Neurobiol.* **44**, 219–229
27. Raper, J. A. (2000) *Curr. Opin. Neurobiol.* **10**, 88–94
28. Chen, H., He, Z., Bagri, A., and Tessier-Lavigne, M. (1998) *Neuron* **21**, 1283–1290
29. Nakamura, F., Tanaka, M., Takahashi, T., Kalb, R. G., and Strittmatter, S. M. (1998) *Neuron* **21**, 1093–1100
30. Renzi, M. J., Feiner, L., Koppel, A. M., and Raper, J. A. (1999) *J. Neurosci.* **19**, 7870–7880
31. Giger, R. J., Urquhart, E. R., Gillespie, S. K. H., Levengood, D. V., Ginty, D. D., and Kolodkin, A. L. (1998) *Neuron* **21**, 1079–1092
32. Romero, A., Romao, M. J., Varela, P. F., Kolln, I., Dias, J. M., Carvalho, A. L., Sanz, L., Topfer-Petersen, E., and Calvete, J. J. (1997) *Nat. Struct. Biol.* **4**, 783–788
33. Takahashi, T., and Strittmatter, S. M. (2001) *Neuron* **29**, 429–439
34. Feiner, L., Webber, A. L., Brown, C. B., Lu, M. M., Jia, L., Feinstein, P., Mombaerts, P., Epstein, J. A., and Raper, J. A. (2001) *Development* **128**, 3061–3070
35. Bagnard, D., Vaillant, C., Khuth, S. T., Dufay, N., Lohrum, M., Puschel, A. W., Belin, M. F., Bolz, J., and Thomasset, N. (2001) *J. Neurosci.* **21**, 3332–3341
36. Sondell, M., Sundler, F., and Kanje, M. (2000) *Eur. J. Neurosci.* **12**, 4243–4254
37. Flanagan, J. G., and Leder, P. (1990) *Cell* **63**, 185–194
38. Motulsky, H. J., and Ransnas, L. A. (1987) *FASEB J.* **1**, 365–374
39. Jones, T. A., Zou, J. Y., Cowan, S. W., and Kjeldgaard. (1991) *Acta Crystallogr. A* **47**, 110–119
40. Brunger, A. T. (1992) *X-PLOR, Version 3.1., a system for x-ray crystallography and NMR*, Yale University Press, New Haven, CT
41. Evans, S. V. (1993) *J. Mol. Graph.* **11**, 127–138